

Article

Not peer-reviewed version

Boldo Restores Vascularization and Reduces Inflammation of Skeletal Muscle in Symptomatic Mice with Dysferlinopathy

[Walter Vásquez](#) ^{*} , [Felipe Troncoso](#) , [Andrea Lira](#) , [Carlos Escudero](#) , [Juan C. Saez](#) ^{*}

Posted Date: 18 August 2025

doi: [10.20944/preprints202508.1188.v1](https://doi.org/10.20944/preprints202508.1188.v1)

Keywords: dysferlinopathy; *Peumus boldus*; skeletal muscle



Preprints.org is a free multidisciplinary platform providing preprint service that is dedicated to making early versions of research outputs permanently available and citable. Preprints posted at Preprints.org appear in Web of Science, Crossref, Google Scholar, Scilit, Europe PMC.

Copyright: This open access article is published under a Creative Commons CC BY 4.0 license, which permit the free download, distribution, and reuse, provided that the author and preprint are cited in any reuse.

Disclaimer/Publisher's Note: The statements, opinions, and data contained in all publications are solely those of the individual author(s) and contributor(s) and not of MDPI and/or the editor(s). MDPI and/or the editor(s) disclaim responsibility for any injury to people or property resulting from any ideas, methods, instructions, or products referred to in the content.

Article

Boldo Restores Vascularization and Reduces Inflammation of Skeletal Muscle in Symptomatic Mice with Dysferlinopathy

Walter Vásquez ^{1,*}, Felipe Troncoso ², Andrea Lira ³, Carlos Escudero ^{2,4} and Juan C. Sáez ^{5,*}

¹ Departamento de Fisiología, Pontificia Universidad Católica de Chile, Santiago, Chile.

² Laboratorio de Fisiología Vascular, Departamento de Ciencias, Universidad del Bío-Bío, Chile

³ Departamento de Morfología, Facultad de Medicina, Universidad Andres Bello, Santiago, Chile

⁴ Group of Research and Innovation in Vascular Health, GRIVAS Health, Chillán, Chile

⁵ Instituto de Neurociencias, Centro Interdisciplinario de Neurociencias de Valparaíso, Universidad de Valparaíso, Valparaíso, Chile

* Correspondence: wavasqueza@gmail.com (W.V.); juancarlos.saez@uv.cl (J.C.S.)

Abstract

Dysferlinopathies are progressive muscular dystrophies caused by mutations in the DYSF gene, leading to defective membrane repair, chronic inflammation, lipid accumulation, and muscle degeneration. No approved therapies currently halt disease progression. This study evaluated the effects of daily oral administration of pulverized Boldo (*Peumus boldus*) leaves, a nutraceutical with reported bioactive properties, in symptomatic blAJ mice, a model of dysferlinopathy. Mice received Boldo for four weeks, and muscle function, vascular performance, histology, and molecular markers were assessed. Boldo treated mice exhibited significantly improved grip strength and restored endothelium dependent vasodilation. Gastrocnemius muscle perfusion and capillary density increased after treatment. Histological analysis revealed prevention of myofiber atrophy, a reduction in centrally nucleated fibers, and improved tissue architecture. Lipid accumulation observed in untreated blAJ mice was absent with Boldo. At the cellular level, Boldo normalized sarcolemmal membrane permeability and decreased mRNA levels of inflammasome components (NLRP3, ASC, IL-1 β), suggesting anti-inflammatory activity. These results indicate that Boldo improves vascular and muscle integrity in dysferlinopathy and support its potential as a complementary therapeutic strategy.

Keywords: dysferlinopathy; *Peumus boldus*; skeletal muscle

1. Introduction

Dysferlin is a 237 kDa membrane protein belonging to the ferlin family, composed of seven C2 domains, one DysF domain, and two Fer domains [1,2]. It is predominantly expressed in the sarcolemma and T-tubules of striated muscles [3,4]. It plays key roles in cell membrane repair [1], and trafficking of membrane proteins [5], affecting vesicle fusion [6], biogenesis of T-tubules, Ca²⁺ signaling [7], phagocytic processes [8], endothelial cell adhesion, repair and angiogenesis [9,10]. Indeed, dysferlin plays a critical role in the repair of the endothelial cell membrane, facilitating the fusion of lysosomes with it, which suggests active involvement in recovery processes and the maintenance of cellular integrity in the endothelium [11]. Specifically, dysferlin regulates endothelial cell adhesion by preventing proteasomal degradation of PECAM-1/CD31, a key adhesion protein for angiogenesis and vascular integrity. Loss of dysferlin impairs endothelial adhesion and angiogenic responses *in vivo*, suggesting a role in maintaining capillary networks and vascular function [9].

Mutations in *DYSF* gene cause a group of muscular dystrophies collectively known as dysferlinopathies, including limb-girdle muscular dystrophy type 2B (LGMDR2) and Miyoshi

myopathy (MM) [10,12,13]. Alterations in the *DYSF* gene are related to a reduction in dysferlin expression and seem to affect the ability of muscle fibers to repair themselves after sarcolemma damage [14]. This process leads to persistent inflammation, muscle degeneration, and the progressive replacement of muscle tissue by fat [15].

Clinically, dysferlinopathies are characterized by a progressive, generally slow decline in motor function of the appendicular system, which usually manifests during adolescence [10,16]. The symptoms are highly variable among individuals, although they tend to develop certain common patterns. Regardless of the appearance of signs of muscle weakness, an increase in serum creatine kinase (CK) levels is characteristic and indicative of muscle damage and has been used for years as a diagnostic criterion in the presence of motor impairment [17].

The presence of distinctive infiltrates of inflammatory cells in skeletal muscle biopsies from patients with dysferlinopathy has been described in the literature, characterized by the presence of macrophages, along with minimal expression of MHC class I molecules (major histocompatibility complex class I) and significant deposition of the complement complex C5b-9, which distinguishes this profile from other inflammatory pathologies [18]. Other studies reported variability in muscle fiber size, confirming the presence of necrotic fibers, regenerative fibers [19,20], an increase in endomysia and perimysium connective tissue, as well as fat accumulation [21].

Leaves of *Peumus boldus*, a Chilean endemic tree called Boldo, contain alkaloids, flavonoids, phenolic acids, and essential oils conferring antioxidant and anti-inflammatory properties [22–24]. Boldine, an active alkaloid present in Boldo leaves, has shown protective effects in animal inflammatory models [25–27], potentially through the blockade of Cx and pannexin-1 hemichannels (Cx HCs and Panx1 HCs, respectively) [28,29]. Boldo is used as a nutraceutical in different countries and its beneficial effects are of popular knowledge that requires scientific support.

On the other hand, the expression of hemichannels constituted of connexins has been observed in skeletal muscle fibers of blAJ mice (model of dysferlinopathy), which was associated with increased sarcolemma permeability and elevated basal intracellular Ca^{2+} signaling [30]. In skeletal muscles affected by dysferlinopathy in humans, an increase in the expression of hemichannels composed of Cx40.1, Cx43, and Cx45 isoforms located in the sarcolemma has been described [31]. Moreover, treatment with boldine normalizes the differentiation fate of myoblasts and features of skeletal muscles from blAJ mice [30]. The de novo Cx HC expression contribute to explain the elevated basal intracellular Ca^{2+} levels observed in dysferlin-deficient myocytes, which was sufficient to disrupt their cellular homeostasis. Therefore, a direct relationship between the absence of dysferlin and the induction of connexin expression has been suggested [31].

Currently, there are no approved therapies that can halt or reverse the progression of dysferlinopathy. Given the multifaceted roles of dysferlin in muscle membrane repair, endothelial adhesion, and angiogenesis, our study aimed to determine whether treatment with boldo, commonly used as nutraceutical, improves muscle function and vascular perfusion, as well as reduces inflammation and lipid infiltration in blAJ mice, a model of dysferlinopathy.

2. Results

2.1. Boldo Improves the Grip Strength and Blood Perfusion in Dysferlinopathy Mice

Dysferlinopathy leads to a gradual decline in muscle strength [32]. Thus, we analyzed the effects of 1 month of daily oral treatment with Boldo and evaluated physical performance using the four-limb suspension test in blAJ mice. Before the intervention, blAJ mice already showed reduced strength compared to WT controls (mean pre-test time: 126.5 ± 17.3 s vs. 195.8 ± 17.1 s, respectively, $n = 4$; $p < 0.01$). WT mice maintained stable performance after one month (post: 223.0 ± 9.7 s), while untreated blAJ mice exhibited a further decline (post: 116.5 ± 17.2 s). In contrast, Boldo-treated blAJ mice showed improved performance (post: 188.0 ± 17.1 s), overcoming their pre-treatment values (139.3 ± 18.3 s). At the end of the treatment period, WT mice performed significantly better than blAJ mice ($p < 0.01$), and Boldo-treated blAJ mice showed a significant improvement compared to

untreated blAJ mice ($p < 0.05$). These results confirm the progressive functional decline in dysferlin-deficient mice and demonstrate that Boldo treatment provides a partial but significant recovery of muscle strength (Figure 1).

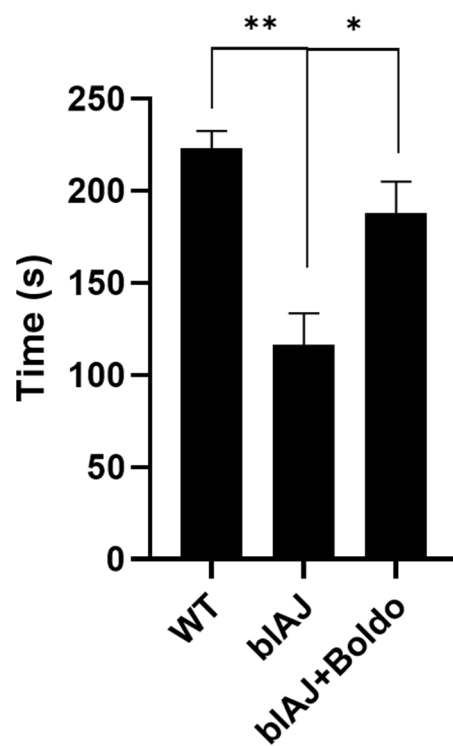


Figure 1. Boldo recovers the physical performance of symptomatic blAJ mice. The physical performance was evaluated using the four-limb suspension test A) Physical performance was assessed in three groups of animals: Wild type (WT); blAJ and blAJ treated with Boldo mice (blAJ + Boldo). n=4. ** $p < 0.01$, * $p < 0.05$, Tukey test.

To determine whether the decline in muscle strength observed in blAJ mice is associated with impaired muscle perfusion, we assessed microvascular blood flow in the gastrocnemius muscle using Laser Doppler imaging (Figures 2A and 2B). blAJ mice exhibited significantly reduced basal perfusion compared to wild-type controls, an effect that was reversed upon treatment with Boldo, as shown in the time-course analysis of perfusion traces (Figure 2B) or in the quantification of average perfusion units (Figure 2C).

To explore whether endothelial dysfunction underlies the perfusion deficit, we evaluated vasodilatory responses to acetylcholine, a classic endothelium-dependent vasodilator. As expected, acetylcholine increased perfusion by approximately 80% over baseline in wild-type mice (Figure 2C). In contrast, this response was markedly blunted in blAJ mice, suggesting impaired endothelial function. Notably, Boldo treatment restored acetylcholine-induced vasodilation in blAJ mice reaching values like the WT mice, supporting a functional recovery of endothelial responsiveness (Figure 2C).

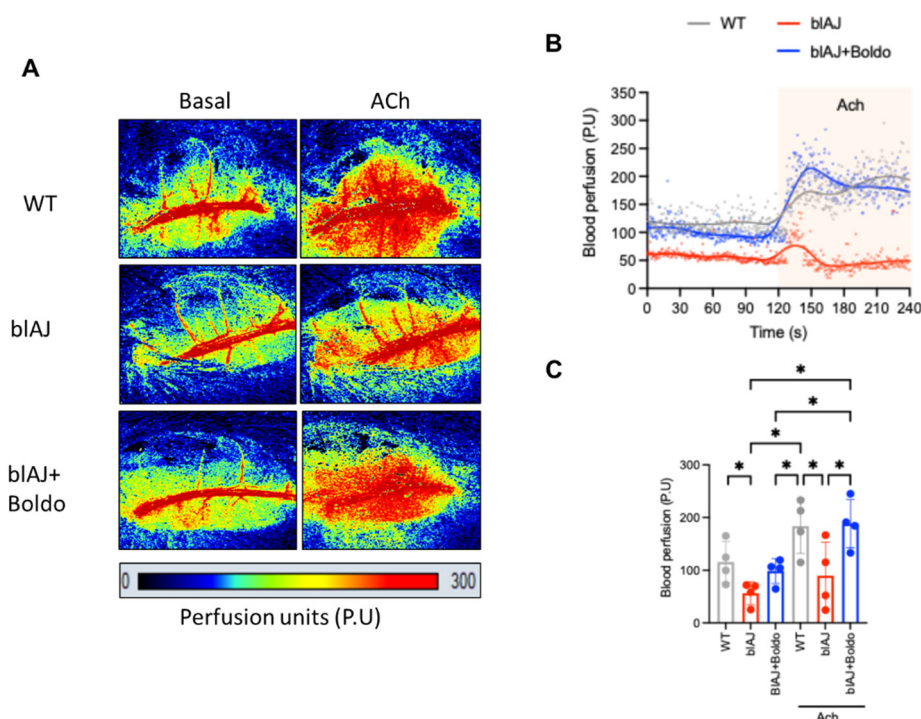


Figure 2. Blood perfusion. A) Representative images of perfusion analysis using Pericam® PSI-HR system in absence (Basal) or in response to acetylcholine (Ach, 10 μ M, topical application) in adult wild type (WT) (WT, gray), blAJ (red), and Boldo-treated blAJ (blue) mice. Perfusion units (arbitrary color units) from 0 to 300. B) Representative trace of blood perfusion from the three experimental groups. Remarked area indicates experiments in presence of Ach. C) Average of four experiments in individual subjects treated as in A. Each dot represents a randomly selected individual subject. Data are presented as median \pm standard deviation. * p <0.05. One-way ANOVA. Multiple comparisons by controlling the False Discovery Rate.

2.2. Boldo Increases Capillary Density in Skeletal Muscle of blAJ Mice

To determine whether the improved blood perfusion observed after Boldo treatment was associated with structural changes in the vasculature, we evaluated the capillary density in gastrocnemius muscle sections using immunofluorescence for CD31, an endothelial cell marker. Compatible with reduced microvascular perfusion blAJ mice exhibited a reduced number of CD31⁺ capillaries per muscle fiber compared to WT mice. Notably, muscles from Boldo-treated blAJ mice showed a partial recovery in capillary density, as evidenced by a higher number of CD31⁺ structures per fiber than untreated blAJ mice (Figure 3B). These results suggest that Boldo may promote vascular remodeling in dysferlin-deficient muscle, potentially contributing to the observed improvements in perfusion and muscle function.

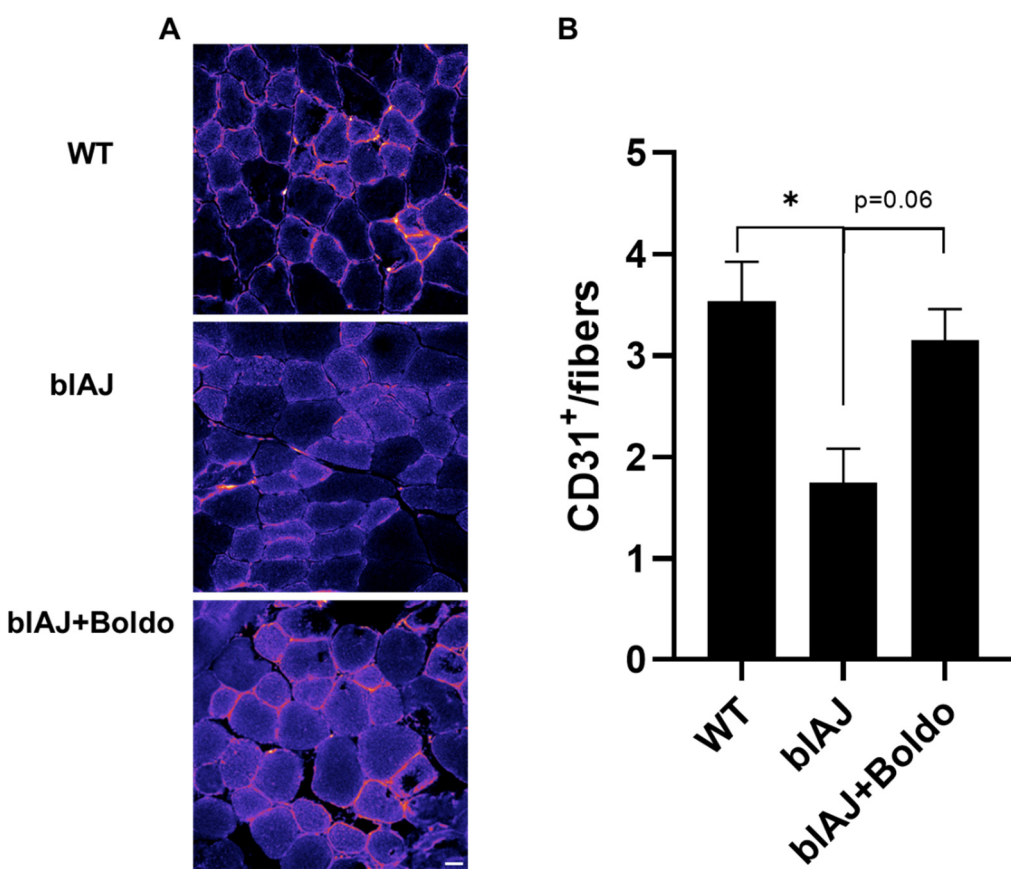


Figure 3. Boldo recovers the capillary density of skeletal muscle from blAJ mice. Representative immunofluorescence images of tibialis anterior muscle cross-sections from wild type (WT), blAJ, and Boldo-treated blAJ mice stained for CD31 (red), an endothelial cell marker. Nuclei were counterstained with DAPI (blue). Quantification of CD31⁺ capillaries per muscle fiber reveals a reduced capillary density in blAJ mice compared to WT, which is partially restored by Boldo treatment. Data are presented as mean \pm SEM. n = 4 mice per group.

Since in blAJ mice the loss of strength is accompanied by muscle atrophy [33]; we evaluated the cross-sectional area of myofibers in the *tibialis anterior* muscles, and found that muscles from blAJ mice presented a clear reduction in CSA of myofibers (~40%) as compared to control muscles (Figure 4B). This reduction was prevented by Boldo treatment as evidence by an increase (~34%) in myofiber cross-sectional area compared to the untreated blAJ mice (Figure 3B). Also, the muscle of blAJ mice presented a significantly higher number of muscle fibers with internal nuclei (~24%), which was less pronounced in the Boldo treated group being close to the values found in muscles of WT mice (Figure 4C).

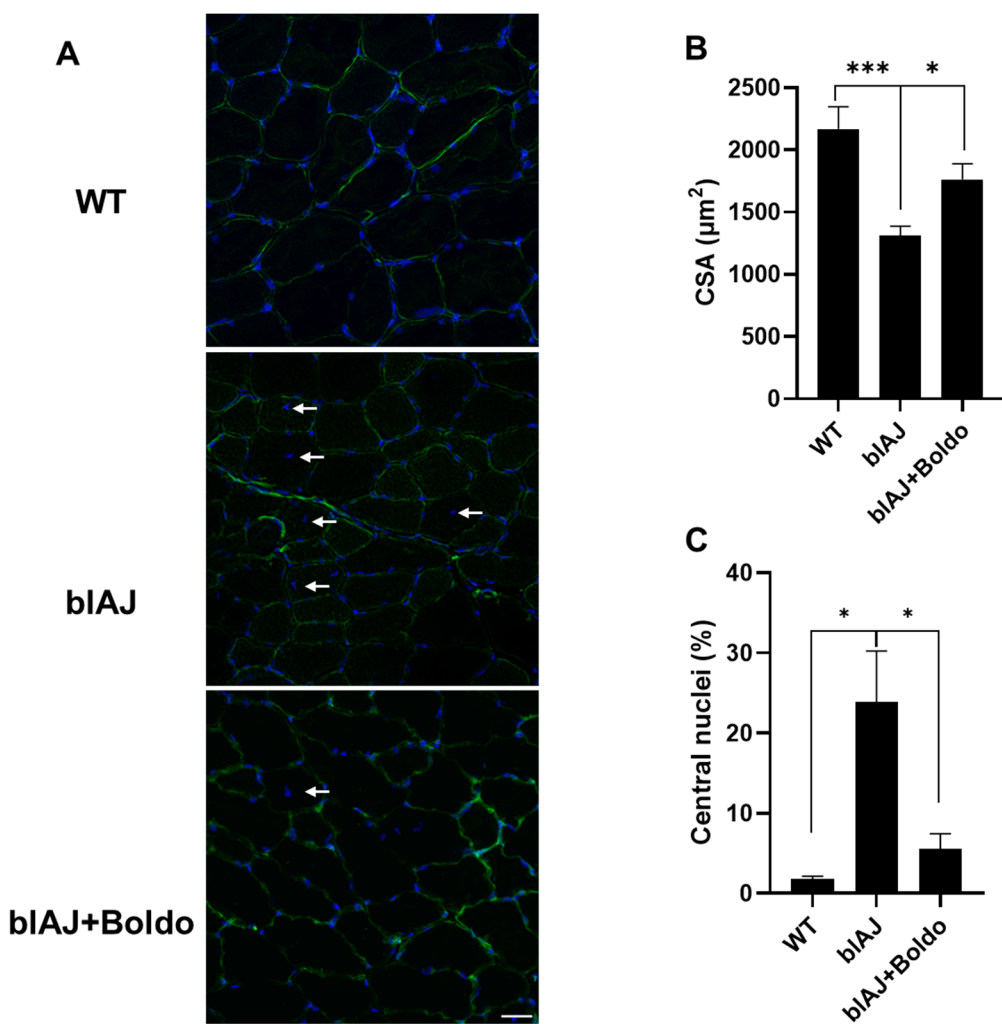


Figure 4. Boldo recovers the cross-section area of *tibialis anterior* myofibers of blAJ mice. A) Distribution of DAPI-stained nuclei (blue) is shown in the middle panel, indicated by white arrowheads. Fiber membranes are labeled with WGA (green). B) Quantification of cross-sectional area (CSA). n=4. ***p<0.001, *p<0.05. Tukey test. C) Quantification of internal nuclei index obtained from DAPI stained muscle cross sections. *p<0.05. Tukey test.

Since the accumulation of lipids within muscles is widely recognized as hallmark of dysferlinopathy [34]. We decided to evaluate whether Boldo can reverse this disease characteristic. To test this possibility, we assessed lipid accumulation in gastrocnemius muscles using Oil Red O staining. While positive staining was observed in muscle sections of blAJ mice, no lipid accumulation was detected in the muscles of WT mice or blAJ mice treated with Boldo (Figure 5A).

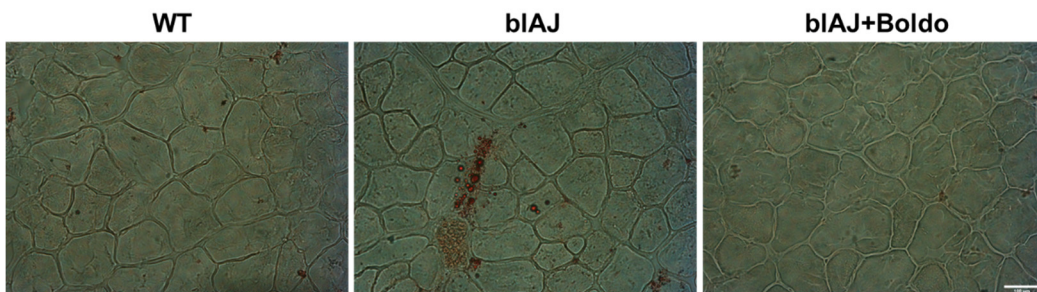


Figure 5. Boldo reduces the lipid accumulation in skeletal muscles of blAJ mice. A) Cryosections of gastrocnemius muscles from wild type (WT), blAJ, and blAJ treated with Boldo mice were analyzed for lipid accumulation using oil red O staining. Scale bar: 100 μm .

2.3. Boldo Improves the Muscular Architecture of bIAJ Mice

Histological examination of tibialis anterior muscle sections stained with hematoxylin and eosin and Masson's Trichrome revealed marked differences between groups (Figure 6). WT mice exhibited uniform polygonal muscle fibers, peripheral nuclei, and intact sarcolemma borders with normal connective tissue distribution. In contrast, bIAJ muscles showed classical dystrophic features, including pronounced fiber size variability, centrally located nuclei, vacuolization, and presence of irregular sarcolemma projections resembling microvilli. These alterations were accompanied by increased cellularity, anisokaryosis, disorganized interstitial architecture, and accumulation of collagen, consistent with chronic degeneration and failed regeneration processes.

Muscles from Boldo treated bIAJ mice displayed partial restoration of tissue architecture. Fiber morphology was more homogeneous, with fewer vacuoles and reduced sarcolemma projections. The number of centrally nucleated fibers was lower, and the extracellular matrix appeared better organized with more regular collagen deposition. These changes suggest that Boldo treatment mitigates the structural deterioration associated with dysferlin deficiency and supports muscle remodeling.

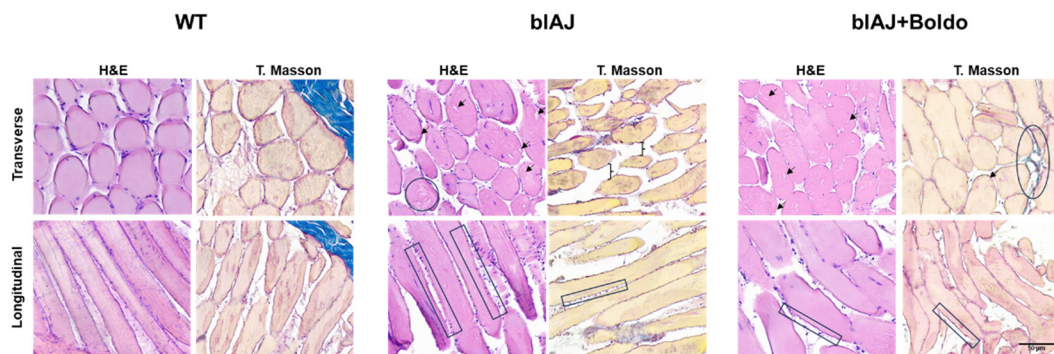


Figure 6. Histopathological analysis of skeletal muscle from WT, bIAJ, and bIAJ mice treated with Boldo. Representative transverse (top row) and longitudinal (bottom row) sections of tibialis anterior muscle stained with hematoxylin and eosin (H&E, left column) or Masson's trichrome (right column). WT muscle displays uniform fiber diameter, peripheral nuclei, and preserved endomysia and perimysium connective tissue. Muscles of bIAJ mice showed dystrophic changes, including fiber size variability, central nuclei, vacuolization (▲), necrotic fibers (●), sarcolemma projections resembling microvilli (□), and epimysia separation (]), along with increased collagen deposition (Masson). Scale bar: 50 μ m.

2.4. Boldo Reduces the Sarcolemma Permeability of Myofibers from bIAJ Mice

Previous studies have demonstrated that myofibers of bIAJ mice express large-pore channels permeable to ions and small molecules [30,33]. Thus, we decided to evaluate the permeability of the sarcolemma in freshly isolated myofibers from FDB muscles. This study was performed by using the ethidium (Etd⁺) uptake assay leakage methods have been widely used to approach the functional state of undocked hemichannels in diverse cellular systems [35].

The fluorescence intensity of myofibers of bIAJ mice increased over time much more than that of myofibers of bIAJ mice treated with Boldo which overlapped with that of myofibers from WT mice (Figure 7A). After five minutes of recording the application of La³⁺ reduced the progressive increase in fluorescence intensity in all myofibers studied (Figure 7A). From these experiments, the Etd⁺ rate of myofibers from bIAJ mice (0.58 ± 0.08 AU/min), was significantly higher than that of the WT group (0.24 ± 0.02 AU/min) (Figure 7B). Importantly, myofibers of Boldo treated bIAJ animals presented dye uptake rate values like myofibers of WT mice (0.31 ± 0.04 AU/min) (Figure 7B).

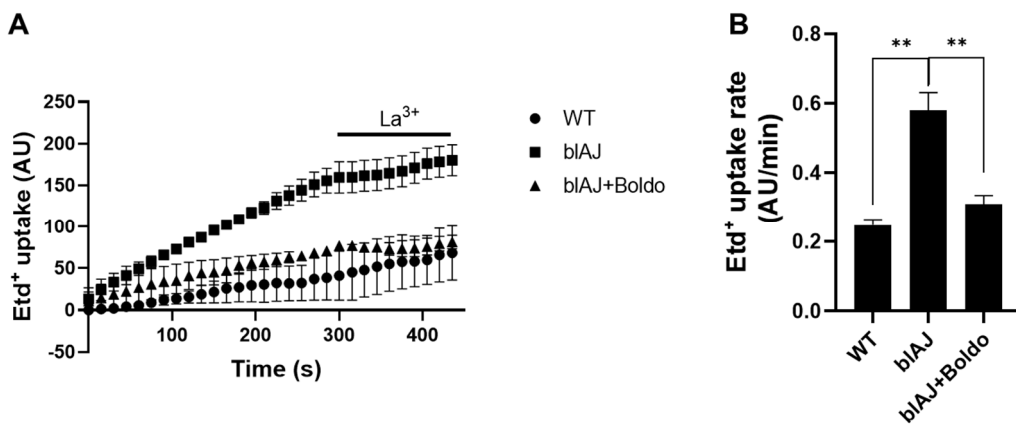


Figure 7. Elevated sarcolemma permeability of freshly isolated blAJ muscle fibers is recovered by Boldo treatment in blAJ mice. A) Representative curve of Etd⁺ uptake over time in isolated myofibers from FDB muscles. B) Etd⁺ uptake rate obtained from slopes of curves similar to A. values represent means \pm SEM. n=4. **p<0.01, Tukey test.

2.5. Boldo Reduces the Levels of Inflammatory Markers in Skeletal Muscles of blAJ Mice

Prior research examined muscle biopsies from control and dysferlin-deficient patients and demonstrated that inflammasome components are present and upregulated in muscles from dysferlin-deficient patients [36]. We evaluated some components of the inflammasome using qPCR. blAJ mice exhibited elevated NLRP3 mRNA levels (2.65 ± 0.98) compared to wild type mice (0.49 ± 0.37), a phenomenon that was prevented with Boldo treatment (0.99 ± 0.32) (Figure 8A). This same behavior was observed in the ASC mRNA levels (Figure 7B) (blAJ mice: 3.23 ± 1.20 and WT: 0.76 ± 0.41 , Boldo treated mice: 1.36 ± 0.79 , respectively) and IL-1 β mRNA levels (Figure 8C), which were significantly elevated in blAJ mice (6.64 ± 1.63) compared to WT (1.07 ± 0.61), and reduced in Boldo-treated blAJ mice (2.23 ± 0.99). Treatment with Boldo significantly reduced the expression of these pro-inflammatory markers, indicating its potential anti-inflammatory effects in dysferlinopathy.

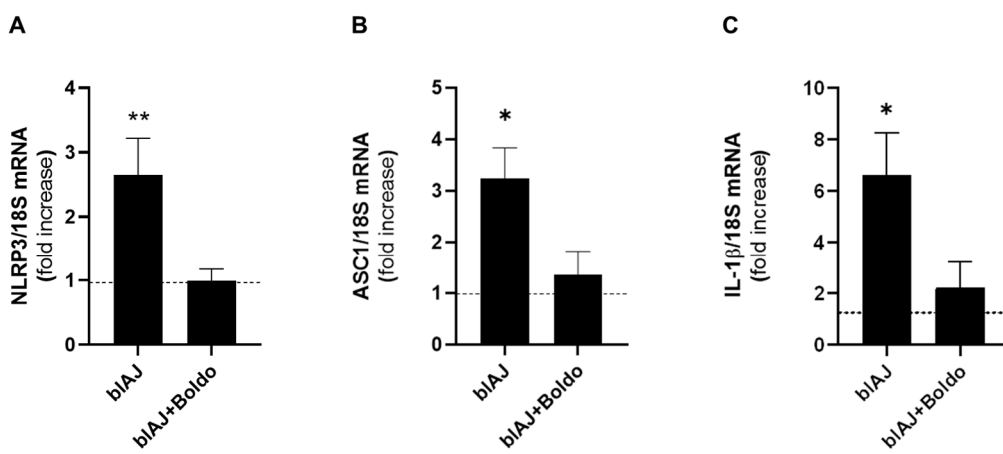


Figure 8. Boldo treatment reduces the mRNA levels of inflammasome components in blAJ mice. Total RNA was isolated from skeletal muscles and mRNA levels of A) NLRP3, B) ASC, and C) IL-1 β were evaluated by qPCR. n=4. **p<0.01, *p<0.05 vs control, Tukey test Dashed line indicates the mean control value.

3. Discussion

In this study, we demonstrated that pulverized Boldo leaves improve physical performance (hanging test), blood perfusion, and vascularization as well as reduce sarcolemma permeabilization,

lipid accumulation and inflammation in skeletal muscles of murine dysferlinopathy model. Currently, this disease has no cure. Therefore, this treatment which consists of the consumption of leaves of a native plant that has not reported side effects, and is accepted as medicinal plant [37,38] could be a complement to improve the current recommended treatments.

Boldo is recognized as a herbal remedy in a number pharmacopoeias and boldine, the main alkaloidal constituent [38], accounts for approximately 0.1% of the total alkaloid content and it is considered the primary bioactive compound [39]. This alkaloid blocks large-pore channels, such as Cx43, Cx45, and Panx1 hemichannels as well as P2X7 receptor [29,40,41]. Recently, symptomatic blAJ mice treated with boldine were shown to present normal muscle performance [30]. Here in, we report similar effects of Boldo-treatment that improved physical performance in the hanging test. These findings raise the possibility that Boldo's effects are mediated by hemichannel blockade, given that dysferlinopathic mice deficient in Cx43 and Cx45 in skeletal muscle retain normal physical performance [33].

In addition to enhancing blood perfusion, we found that Boldo treatment partially restores capillary density in skeletal muscle of blAJ mice. Dysferlin deficiency has previously been associated with reduced capillary density and impaired angiogenic responses due to endothelial dysfunction and defective PECAM-1 stabilization [9]. Consistently, we observed a reduction in the number of CD31⁺ capillaries per fiber in blAJ mice, which was partially reversed by Boldo. This increase in capillary density suggests that Boldo may preserve or promote vascular integrity in dystrophic muscle. Similar vascular abnormalities have been found in other muscular dystrophies, including Duchenne muscular dystrophy, where reduced capillary density contributes to tissue hypoxia and exacerbates muscle damage [42]. Therefore, the ability of Boldo to restore vascularization could represent an additional mechanism by which it protects skeletal muscle in dysferlinopathy.

The decrease in physical performance in this disease is associated with muscle atrophy, characterized by a decrease in the CSA of muscle fibers [33,43]. Notably, the use of Boldo reverses the CSA of skeletal myofibers in blAJ mice. Also, an important histopathological feature of dysferlinopathy is the presence of centrally located nuclei within muscle fibers, indicative of ongoing cycles of degeneration and regeneration [44]. We found that Boldo treatment reduces the number of centrally nucleated myofibers in blAJ mice, suggesting a reduction in continuous cell death and regeneration process.

Also, extensive fatty infiltration of myofibers in patients with dysferlinopathy has been observed through imaging techniques such as magnetic resonance imaging [45]. In one reported case of limb-girdle muscular dystrophy type 2B due to dysferlin deficiency, the lumbar and lower thoracic portions of the erector spinae muscles were entirely filled with fatty vesicles [46]. The same occurs in animal models such as A/Jdys^{-/-} and blAJ that report lipid accumulation in skeletal muscle [34]. Interestingly, we found that treatment with Boldo decreased lipid accumulation in skeletal muscle of blAJ mice. Since this fat accumulation does not occur in blAJ mice with myofibers deficient in Cx43 and Cx45 [33], a proposed explanation for this lipid accumulation is the propensity of muscle myogenic cells to adopt an adipogenic phenotype. Accordingly, a human dysferlinopathy myoblast cell line, cultured under conditions that promote myogenic differentiation, manifests aberrant adipogenic commitment, as indicated by PPAR γ expression [30]. This phenomenon accounts for the increased number of Oil Red O-positive cells and the reduced formation of myotubes observed at later stages of differentiation. Notably, treatment with boldine effectively reversed this aberrant adipogenic commitment, reducing PPAR γ expression, decreasing lipid accumulation, and restoring myotube formation capacity [30]. In addition to the effect on progenitor cell fate, the reduction in lipid accumulation may also result from the progressive degeneration and removal of previously lipid-laden muscle fibers [47]. As these damaged fibers are replaced by newly regenerated myofibers formed under conditions of improved perfusion and lower inflammation the new muscle tissue lacks the aberrant lipid content, thereby contributing to the overall decrease in intramuscular fat observed after Boldo treatment.

The increase in sarcolemma permeability observed in the muscle fibers of blAJ mice is mediated, at least in part, by the expression of large-pore channels such as Cx43 and Cx45 hemichannels. Previous studies have shown that blAJ mice deficient in Cx43 and Cx45 exhibit absence of elevated sarcolemma permeability, indicating that the absence of these connexins is sufficient to mitigate the rise in membrane permeability [33]. Here, treatment with Boldo was found to cause a similar increase in sarcolemma permeability of myofibers of blAJ mice. These findings parallel the results observed in myofibers of blAJ mice deficient in Cx43 and Cx45 expression, suggesting that Boldo may exert its protective action by modulating the activity and/or expression of these non-selective channels.

Cx43 HCs P2X7 receptor and TRPV2 channel are present in muscular biopsies from dysferlinopathy patients [31] and are permeable to Ca^{2+} [48–50]. Thus, all of them can contribute to a sustained increase in cytoplasmic Ca^{2+} levels [31,33]. Additionally, Cx HCs mediate the efflux of ATP into the extracellular space [51], where it can activate ionotropic purinergic receptors (P2X receptors resulting in further Ca^{2+} constituting a feedforward mechanism that activate the inflammasome complex [52]. This sequence of events promotes a chronic inflammatory state, which is a well-established feature of dysferlinopathy [53–55].

Supporting the relevance of inflammasome activation in dysferlinopathy, previous studies have shown increased levels of NLRP3, ASC, active caspase-1, and mature IL-1 β in the skeletal muscles of dysferlin-deficient (A/J) mice [36]. Myotubes from primary myoblast cultures of these animals also expressed these components, confirming that muscle cells alone can assemble a functional inflammasome and secrete IL-1 β , a key cytokine driving chronic inflammation [36]. In line with these reports, we also observed elevated expression of inflammasome-related components, including ASC, NLRP3, and IL-1 β , as determined by qPCR analysis in skeletal muscle of blAJ mice. Interestingly, Boldo treatment significantly reduced the levels of these markers, further supporting its role in dampening inflammasome-mediated inflammation in dysferlinopathy.

In conclusion, our findings indicate that Boldo improves vascular and muscle integrity and supports its potential as a complementary therapeutic strategy for dysferlinopathy. Building on these results, we highlight Boldo's potential as a therapeutic agent for dysferlinopathy, contingent on standardized dosage, administration, and treatment duration. The animals included in this study were symptomatic blAJ mice, which reinforces the translational relevance of our findings. Therefore, we advocate for future clinical investigations to evaluate Boldo as a therapy, which is supported by the lack of toxicity and its use in clinical trial for treating overactive bladder in women (National Library of Medicine).

4. Materials and Methods

4.1. Reagents

Ethidium (Et d^+) bromide, DMEM/F12 medium and FBS were purchased from GIBCO/BRL (Grand Island, NY, USA). Fluoromount-G and 4 ',6-diamidino-2-fenilindol (DAPI) were obtained from Science (Hatfield, PA, USA).

4.2. Animals

This proposal used males from wild type C57Bl/6 background and blAJ mice (dysferlin-deficient animals). These animals bear a homozygous mutation in both alleles of the DYSF gene and present several muscle alterations characteristic of this type of muscular dystrophy. All protocols were approved by the Bioethics Committee of the Universidad de Valparaíso in accordance with the ethical standards established in the 1964 Declaration of Helsinki and its later amendments. All efforts were made to minimize animal suffering and to reduce the number of animals used, and alternatives to *in vivo* techniques were implemented when it was possible.

4.3. Boldo Treatment

The different mice strains used in this work were treated with pulverized Boldo (*Peumus boldus*) leaves (50 mg/kg, daily) for 4 weeks. Boldo (Té Supremo from Chile) was administered to mice mixed with 3 mg of peanut butter in a separate cage (one mouse at the time).

4.4. Blood Perfusion

In vivo muscle perfusion was assessed using the Pericam® PSI-HR system (Perimed Ltd., Stockholm, Sweden). Adult mice were anesthetized with 4% isoflurane, and the skin over the right gastrocnemius muscle was carefully removed to expose the microvasculature. Microvascular blood flow was recorded from four predefined circular regions of interest (ROIs) within the muscle, consistently positioned across animals to capture representative microcirculation.

The experimental protocol included a 3–4 minutes baseline perfusion recording, followed by a single bolus of acetylcholine (10 μ M) to induce endothelium-dependent vasodilation. Continuous perfusion monitoring was maintained throughout the experiment (~10 minutes). For quantification, time-of-interest (TOI) windows of 40 seconds were extracted for both basal and post-acetylcholine conditions, beginning immediately after drug administration. Perfusion values are reported in raw perfusion units.

Data acquisition and analysis were conducted by two independent investigators (FT and HS). To minimize bias, experiments were performed in a randomized, head-to-head fashion, simultaneously including mice from all experimental groups. Data analysis was performed in a blinded manner.

4.5. Muscular Force Test

The four-limb suspension test was used to assess muscle strength in mice. Animals were placed on a wire grid at a height of 35 cm, with a soft bed underneath to prevent injury in case of a fall. Suspension time was recorded in seconds. Each mouse performed several trials, with 2-minute rest intervals between each trial.

4.6. Histology

Muscle samples were fixed with 4% paraformaldehyde for 48 hours at 4°C. Subsequently, those samples were dehydrated in alcohol baths and then embedded in paraffin. Sections of 5 μ m thickness were cut using a microtome (Accu-Cut® SRM™ 200, Sakura Finetek). Finally, histological stains using Hematoxylin and Eosin (H&E) were performed to observe variations in tissue architecture. Masson's Trichrome staining was used for collagen fibers analysis. For the Masson's Trichrome staining, Weigert's hematoxylin was used for nuclear staining, followed by a Biebrich Scarlet solution (acidic fuccina at 1%, Biebrich Scarlet at 1%, and glacial acetic acid) for cytoplasmic staining for 10 seconds. Then, a mordant solution of phosphotungstic/phosphomolybdic acid was applied for 15 minutes. Finally, to highlight the collagen fibers, an aniline blue solution (aniline blue, acetic acid, and distilled water) was used. All images were captured with a 40X objective using an optical microscope (Olympus CX43RF) equipped with a digital camera (Euromex 4K Sony Ultra HD VC.3040).

4.7. Cross Sectional Area

This parameter was evaluated in tibialis anterior (TA) muscle fibers. Muscles were fixed in 4% (wt/vol) paraformaldehyde, fast frozen in isopentane maintained in liquid nitrogen. Then, muscles were oriented perpendicular and mounted in OCT. Cross sections (10 μ m thick) of frozen muscles were obtained using a cryostat (Leica CM1100) e with ImageJ software (National Institutes of Health)

4.8. Immunofluorescence Analysis

Muscles were fast frozen with in liquid nitrogen. Then, cross-sections (12 μ m thick) were obtained by using a cryostat and fixed with 4% formaldehyde for 10 min at room temperature. Sections were incubated for 3 h at room temperature in blocking solution (50 mM NH₄Cl, 0.025% Triton, 1% BSA on PBS solution 1 \times), incubated overnight with appropriate dilutions of primary antibody directed to CD31, washed five times with PBS 1 \times solution followed by 1 h incubation with secondary rabbit antibody conjugated to Cy2 or Cy3 were purchased from Jackson ImmunoResearch Laboratories (West Grove, PA, USA), and mounted in Fluoromount G from Electron Microscopy Science (Hatfield, PA, USA). Immunoreactive binding sites were localized under a Nikon Eclipse Ti microscope equipped with epifluorescence illumination.

4.9. Oil Red O Staining

This staining was carried out as previously described [56]. Briefly, cross sections of gastrocnemius muscles mounted on glass slides were fixed with 4% paraformaldehyde in the presence of 180 mM CaCl₂. After that, oil red O reagent was added and after 30 min the excess was removed, and the samples were rinsed with water.

4.10. Isolation of Mouse Skeletal Myofibers

Myofibers were isolated from flexor digitorum brevis (FDB) muscles as previously described [40]. FDB muscles were carefully dissected and immersed in culture medium (DMEM/F12 supplemented with 10% FBS) containing 0.2% collagenase type I, incubated for 3 h at 37°C, and transferred to a 15 mL test tube (Falcon) with 5 mL of culture medium. Then, muscle tissue was gently triturated 10 times by using a Pasteur pipette with a wide tip to disperse single myofibers. Dissociated myofibers were centrifuged at 1,000 rpm for 15 s (model 8700 centrifuge; Kubota) and washed twice by sedimentation, first in PBS solution and then in Krebs buffer (in mM: 145 NaCl, 5 KCl, 3 CaCl₂, 1 MgCl₂, 5.6 glucose, 10 HEPES-Na, pH 7.4), the latter containing 10 μ M BTS to inhibit contractions and to reduce myofiber damage during the isolation procedure. Finally, fibers were suspended in 5 mL of Krebs HEPES buffer with 10 μ M BTS, plated in plastic culture dishes or placed in 1.5 mL microcentrifuge tubes, and kept at room temperature.

4.11. Time-Lapse Recording of Etd⁺ Uptake

Cellular uptake of Etd⁺ was evaluated by time-lapse measurements as previously described [40]. Briefly, freshly isolated myofibers plated onto plastic culture dishes were washed twice with Krebs buffer solution containing 5 μ M Etd⁺. The Etd⁺ fluorescence intensity was recorded in regions of interest that corresponded to myofiber nuclei by using a conventional Nikon Eclipse Ti fluorescent microscope.

4.12. Reverse Transcription Polymerase Chain Reaction (PCR)

Total RNA was isolated from skeletal muscle using TRIzol following the manufacturer's instructions (Invitrogen, Waltham, MA, USA). Two microgram aliquots of total RNA were transcribed to cDNA using MMLV-reverse transcriptase (Fermentas, USA), and mRNA levels were evaluated by PCR amplification (GoTaq Flexi DNA polymerase; Promega, USA).

4.13. The Oligos Used Were the Following

NLRP3: S 5'- GCTGGCATCTGGGGAAACCT-3', AS 5'GCCCTTCTGGGGAGGATAGT-3'; IL-1 β : S 5'- TGG GAT GAT GAT AAC CT -3', AS 5'-CCC ATA CTT TAG GAA GAC AGG GAT TT-3'; 18S S 5'- TCAAGAACGAAAGTCGGAGG-3', AS 5'-GGACATCTAAGGGCATCACA-3'. All reactions were performed with an initial denaturation of 5 min at 95°C, followed by 40 cycles of 30 s at 95°C, and annealing for 30 s at 60°C in a PikoReal™ Real-Time PCR System (ThermoFisher

Scientific™). Ct values of each cDNA resulting from three different experiments were normalized using the $2^{-\Delta\Delta Ct}$ method, with 18S serving as the reference gene.

4.14. Statistical Analysis

Quantitative variables are presented as median \pm standard deviation. Considering data distribution, we used parametric or non-parametric tests, as appropriate, using the Shapiro-Wilk normality test. For multiple groups comparison during perfusion analysis data is presented as mean value calculated from four different subjects. Multiple comparison was performed using ordinary one-way ANOVA followed by multiple comparison by controlling the False Discovery Rate by using the f Benjamini and Hockberg's method. In other experiments, data were analyzed using one-way ANOVA followed by Tukey's multiple comparisons test, accordingly with normality test. P<0.05 was considered a statistically significant difference. Data and statistical analyses were performed using the Microsoft Excel database and GraphPad Prism 6 (GraphPad Software, CA, USA).

Author Contributions: Conceptualization, W.V. and J.C.S.; methodology, W.V., F.T., A.L., C.E. and J.C.S.; software, W.V and F.T.; validation, W.V., F.T., A.L., C.E. and J.C.S.; formal analysis, W.V. and J.C.S.; investigation, W.V., F.T., A.L., C.E. and J.C.S.; resources, C.E. and J.C.S.; writing—original draft preparation, W.V., and J.C.S.; writing—review and editing, W.V., F.T., A.L., C.E. and J.C.S.; visualization, W.V and J.C.S.; supervision, J.C.S.; project administration, J.C.S.; funding acquisition, C.E. and J.C.S. All authors have read and agreed to the published version of the manuscript.

Funding: This work was partially funded by ANID projects 1231523 (to J.C.S.) and a Doctoral fellowship from ANID 21211179 (W.V.) and 21241885 (A.L.) The experimental data in this paper are from a thesis submitted in partial fulfillment of the requirements for the Doctorate in Biological Sciences, mention Physiological Science (W.V.) at Pontificia Universidad Católica de Chile. CE is founded by Fondecyt 1240295 and GI2301146.

Conflicts of Interest: The authors declare no conflicts of interest.

References

1. Bansal, D.; Miyake, K.; Vogel, S.S.; Groh, S.; Chen, C.-C.; Williamson, R.; McNeil, P.L.; Campbell, K.P. Defective Membrane Repair in Dysferlin-Deficient Muscular Dystrophy. *Nature* **2003**, *423*, 168–172, doi:10.1038/nature01573.
2. Matsuda, C.; Hayashi, Y.K.; Ogawa, M.; Aoki, M.; Murayama, K.; Nishino, I.; Nonaka, I.; Arahata, K.; Brown, R.H. The Sarcolemmal Proteins Dysferlin and Caveolin-3 Interact in Skeletal Muscle. *Hum. Mol. Genet.* **2001**, *10*, 1761–1766, doi:10.1093/hmg/10.17.1761.
3. Anderson, L.V.; Davison, K.; Moss, J.A.; Young, C.; Cullen, M.J.; Walsh, J.; Johnson, M.A.; Bashir, R.; Britton, S.; Keers, S.; et al. Dysferlin Is a Plasma Membrane Protein and Is Expressed Early in Human Development. *Hum. Mol. Genet.* **1999**, *8*, 855–861, doi:10.1093/hmg/8.5.855.
4. McDade, J.R.; Archambeau, A.; Michele, D.E. Rapid Actin-Cytoskeleton-Dependent Recruitment of Plasma Membrane-Derived Dysferlin at Wounds Is Critical for Muscle Membrane Repair. *FASEB J.* **2014**, *28*, 3660–3670, doi:10.1096/fj.14-250191.
5. Leung, C.; Utokaparch, S.; Sharma, A.; Yu, C.; Abraham, T.; Borchers, C.; Bernatchez, P. Proteomic Identification of Dysferlin-Interacting Protein Complexes in Human Vascular Endothelium. *Biochem. Biophys. Res. Commun.* **2011**, *415*, 263–269, doi:10.1016/j.bbrc.2011.10.031.
6. Davenport, N.R.; Sonnemann, K.J.; Eliceiri, K.W.; Bement, W.M. Membrane Dynamics during Cellular Wound Repair. *Mol. Biol. Cell* **2016**, *27*, 2272–2285, doi:10.1091/mbc.E16-04-0223.
7. Muriel, J.; Lukyanenko, V.; Kwiatkowski, T.; Bhattacharya, S.; Garman, D.; Weisleder, N.; Bloch, R.J. The C2 Domains of Dysferlin: Roles in Membrane Localization, Ca²⁺ Signalling and Sarcolemmal Repair. *J. Physiol.* **2022**, *600*, 1953–1968, doi:10.1113/JP282648.
8. Cárdenas, A.M.; González-Jamett, A.M.; Cea, L.A.; Bevilacqua, J.A.; Caviedes, P. Dysferlin Function in Skeletal Muscle: Possible Pathological Mechanisms and Therapeutic Targets in Dysferlinopathies. *Exp. Neurol.* **2016**, *283*, 246–254, doi:10.1016/j.expneurol.2016.06.026.

9. Sharma, A.; Yu, C.; Leung, C.; Trane, A.; Lau, M.; Utokaparch, S.; Shaheen, F.; Sheibani, N.; Bernatchez, P. A New Role for the Muscle Repair Protein Dysferlin in Endothelial Cell Adhesion and Angiogenesis. *Arterioscler. Thromb. Vasc. Biol.* **2010**, *30*, 2196–2204, doi:10.1161/ATVBAHA.110.208108.
10. Urtizberea, J.A.; Bassez, G.; Leturcq, F.; Nguyen, K.; Krahn, M.; Levy, N. Dysferlinopathies. *Neurol. India* **2008**, *56*, 289, doi:10.4103/0028-3886.43447.
11. Han, R. Muscle Membrane Repair and Inflammatory Attack in Dysferlinopathy. *Skelet. Muscle* **2011**, *1*, 10, doi:10.1186/2044-5040-1-10.
12. Bashir, R.; Britton, S.; Strachan, T.; Keers, S.; Vafiadaki, E.; Lako, M.; Richard, I.; Marchand, S.; Bourg, N.; Argov, Z.; et al. A Gene Related to Caenorhabditis Elegans Spermatogenesis Factor Fer-1 Is Mutated in Limb-Girdle Muscular Dystrophy Type 2B. *Nat. Genet.* **1998**, *20*, 37–42, doi:10.1038/1689.
13. Laval, S.H.; Bushby, K.M.D. Limb-Girdle Muscular Dystrophies--from Genetics to Molecular Pathology. *Neuropathol. Appl. Neurobiol.* **2004**, *30*, 91–105, doi:10.1111/j.1365-2990.2004.00555.x.
14. González-Jamett, A.; Vásquez, W.; Cifuentes-Riveros, G.; Martínez-Pando, R.; Sáez, J.C.; Cárdenas, A.M. Oxidative Stress, Inflammation and Connexin Hemichannels in Muscular Dystrophies. *Biomedicines* **2022**, *10*, 507, doi:10.3390/biomedicines10020507.
15. Defour, A.; Medikayala, S.; Van der Meulen, J.H.; Hogarth, M.W.; Holdreith, N.; Malatras, A.; Duddy, W.; Boehler, J.; Nagaraju, K.; Jaiswal, J.K. Annexin A2 Links Poor Myofiber Repair with Inflammation and Adipogenic Replacement of the Injured Muscle. *Hum. Mol. Genet.* **2017**, *26*, 1979–1991, doi:10.1093/hmg/ddx065.
16. Bouchard, C.; Tremblay, J.P. Portrait of Dysferlinopathy: Diagnosis and Development of Therapy. *J. Clin. Med.* **2023**, *12*, 6011, doi:10.3390/jcm12186011.
17. Ivanova, A.; Smirnikhina, S.; Lavrov, A. Dysferlinopathies: Clinical and Genetic Variability. *Clin. Genet.* **2022**, *102*, 465–473, doi:10.1111/cge.14216.
18. Becker, N.; Moore, S.A.; Jones, K.A. The Inflammatory Pathology of Dysferlinopathy Is Distinct from Calpainopathy, Becker Muscular Dystrophy, and Inflammatory Myopathies. *Acta Neuropathol. Commun.* **2022**, *10*, 17, doi:10.1186/s40478-022-01320-z.
19. Selcen, D.; Stilling, G.; Engel, A.G. The Earliest Pathologic Alterations in Dysferlinopathy. *Neurology* **2001**, *56*, 1472–1481, doi:10.1212/wnl.56.11.1472.
20. Wang, Y.; Lu, J.; Liu, Y. Skeletal Muscle Regeneration in Cardiotoxin-Induced Muscle Injury Models. *Int. J. Mol. Sci.* **2022**, *23*, 13380, doi:10.3390/ijms232113380.
21. Fernández-Eulate, G.; Querin, G.; Moore, U.; Behin, A.; Masingue, M.; Bassez, G.; Leonard-Louis, S.; Laforêt, P.; Maisonneuve, T.; Merle, P.-E.; et al. Deep Phenotyping of an International Series of Patients with Late-Onset Dysferlinopathy. *Eur. J. Neurol.* **2021**, *28*, 2092–2102, doi:10.1111/ene.14821.
22. Fernández, J.; Lagos, P.; Rivera, P.; Zamorano-Ponce, E. Effect of Boldo (Peumus Boldus Molina) Infusion on Lipoperoxidation Induced by Cisplatin in Mice Liver. *Phytother. Res. PTR* **2009**, *23*, 1024–1027, doi:10.1002/ptr.2746.
23. Ferrante, C.; Chiavaroli, A.; Angelini, P.; Venanzoni, R.; Angeles Flores, G.; Brunetti, L.; Petrucci, M.; Politi, M.; Menghini, L.; Leone, S.; et al. Phenolic Content and Antimicrobial and Anti-Inflammatory Effects of Solidago Virga-Aurea, Phyllanthus Niruri, Epilobium Angustifolium, Peumus Boldus, and Ononis Spinosa Extracts. *Antibiot. Basel Switz.* **2020**, *9*, 783, doi:10.3390/antibiotics9110783.
24. Schmeda-Hirschmann, G.; Rodriguez, J.A.; Theoduloz, C.; Astudillo, S.L.; Feresin, G.E.; Tapia, A. Free-Radical Scavengers and Antioxidants from Peumus Boldus Mol. (“Boldo”). *Free Radic. Res.* **2003**, *37*, 447–452, doi:10.1080/1071576031000090000.
25. Backhouse, N.; Delporte, C.; Givernau, M.; Cassels, B.K.; Valenzuela, A.; Speisky, H. Anti-Inflammatory and Antipyretic Effects of Boldine. *Agents Actions* **1994**, *42*, 114–117, doi:10.1007/BF01983475.
26. Shuker, E.; Farhood, M.; Al-Qudaihi, G.; Fouad, D. Potential Effects of Boldine on Oxidative Stress, Apoptosis, and Inflammatory Changes Induced by the Methylprednisolone Hepatotoxicity in Male Wistar Rats. *Dose-Response Publ. Int. Hormesis Soc.* **2022**, *20*, 15593258221082877, doi:10.1177/15593258221082877.
27. Yang, X.; Gao, X.; Cao, Y.; Guo, Q.; Li, S.; Zhu, Z.; Zhao, Y.; Tu, P.; Chai, X. Anti-Inflammatory Effects of Boldine and Reticuline Isolated from Litsea Cubeba through JAK2/STAT3 and NF-κB Signaling Pathways. *Planta Med.* **2018**, *84*, 20–25, doi:10.1055/s-0043-113447.

28. Hernández-Salinas, R.; Vielma, A.Z.; Arismendi, M.N.; Boric, M.P.; Sáez, J.C.; Velarde, V. Boldine Prevents Renal Alterations in Diabetic Rats. *J. Diabetes Res.* **2013**, *2013*, 593672, doi:10.1155/2013/593672.

29. Yi, C.; Ezan, P.; Fernández, P.; Schmitt, J.; Sáez, J.C.; Giaume, C.; Koulakoff, A. Inhibition of Glial Hemichannels by Boldine Treatment Reduces Neuronal Suffering in a Murine Model of Alzheimer's Disease. *Glia* **2017**, *65*, 1607–1625, doi:10.1002/glia.23182.

30. Cea, L.A.; Fernández, G.; Arias-Bravo, G.; Castillo-Ruiz, M.; Escamilla, R.; Brañes, M.C.; Sáez, J.C. Blockade of Hemichannels Normalizes the Differentiation Fate of Myoblasts and Features of Skeletal Muscles from Dysferlin-Deficient Mice. *Int. J. Mol. Sci.* **2020**, *21*, doi:10.3390/ijms21176025.

31. Cea, L.A.; Bevilacqua, J.A.; Arriagada, C.; Cárdenas, A.M.; Bigot, A.; Mouly, V.; Sáez, J.C.; Caviedes, P. The Absence of Dysferlin Induces the Expression of Functional Connexin-Based Hemichannels in Human Myotubes. *BMC Cell Biol.* **2016**, *17*, doi:10.1186/s12860-016-0096-6.

32. Lloyd, E.M.; Crew, R.C.; Haynes, V.R.; White, R.B.; Mark, P.J.; Jackaman, C.; Papadimitriou, J.M.; Pinniger, G.J.; Murphy, R.M.; Watt, M.J.; et al. Pilot Investigations into the Mechanistic Basis for Adverse Effects of Glucocorticoids in Dysferlinopathy. *Skelet. Muscle* **2024**, *14*, 19, doi:10.1186/s13395-024-00350-6.

33. Fernández, G.; Arias-Bravo, G.; Bevilacqua, J.A.; Castillo-Ruiz, M.; Caviedes, P.; Sáez, J.C.; Cea, L.A. Myofibers Deficient in Connexins 43 and 45 Expression Protect Mice from Skeletal Muscle and Systemic Dysfunction Promoted by a Dysferlin Mutation. *Biochim. Biophys. Acta Mol. Basis Dis.* **2020**, *1866*, 165800, doi:10.1016/j.bbadi.2020.165800.

34. Grounds, M.D.; Terrill, J.R.; Radley-Crabb, H.G.; Robertson, T.; Papadimitriou, J.; Spuler, S.; Shavlakadze, T. Lipid Accumulation in Dysferlin-Deficient Muscles. *Am. J. Pathol.* **2014**, *184*, 1668–1676, doi:10.1016/j.ajpath.2014.02.005.

35. Johnson, R.G.; Le, H.C.; Evenson, K.; Loberg, S.W.; Myslajek, T.M.; Prabhu, A.; Manley, A.-M.; O'Shea, C.; Grunenwald, H.; Haddican, M.; et al. Connexin Hemichannels: Methods for Dye Uptake and Leakage. *J. Membr. Biol.* **2016**, *249*, 713–741, doi:10.1007/s00232-016-9925-y.

36. Rawat, R.; Cohen, T.V.; Ampong, B.; Francia, D.; Henriques-Pons, A.; Hoffman, E.P.; Nagaraju, K. Inflammasome Up-Regulation and Activation in Dysferlin-Deficient Skeletal Muscle. *Am. J. Pathol.* **2010**, *176*, 2891–2900, doi:10.2353/ajpath.2010.090058.

37. Russo, A.; Cardile, V.; Caggia, S.; Gunther, G.; Troncoso, N.; Garbarino, J. Boldo Prevents UV Light and Nitric Oxide-Mediated Plasmid DNA Damage and Reduces the Expression of Hsp70 Protein in Melanoma Cancer Cells. *J. Pharm. Pharmacol.* **2011**, *63*, 1219–1229, doi:10.1111/j.2042-7158.2011.01320.x.

38. Speisky, H.; Cassels, B.K. Boldo and Boldine: An Emerging Case of Natural Drug Development. *Pharmacol. Res.* **1994**, *29*, 1–12, doi:10.1016/1043-6618(94)80093-6.

39. Fuentes-Barros, G.; Echeverría, J.; Mattar, C.; Liberona, L.; Giordano, A.; Suárez-Rozas, C.; Salas-Norambuena, J.; González-Cooper, A.; Cassels, B.K.; Castro-Saavedra, S. Phytochemical Variation of Wild and Farmed Populations of Boldo (*Peumus Boldus Molina*). *J. Appl. Res. Med. Aromat. Plants* **2023**, *35*, 100502, doi:10.1016/j.jarmap.2023.100502.

40. Cea, L.A.; Vásquez, W.; Hernández-Salinas, R.; Vielma, A.Z.; Castillo-Ruiz, M.; Velarde, V.; Salgado, M.; Sáez, J.C. Skeletal Muscle Atrophy Induced by Diabetes Is Mediated by Non-Selective Channels and Prevented by Boldine. *Biomolecules* **2023**, *13*, 708, doi:10.3390/biom13040708.

41. Toro, C.A.; Johnson, K.; Hansen, J.; Siddiq, M.M.; Vásquez, W.; Zhao, W.; Graham, Z.A.; Sáez, J.C.; Iyengar, R.; Cardozo, C.P. Boldine Modulates Glial Transcription and Functional Recovery in a Murine Model of Contusion Spinal Cord Injury. *Front. Cell. Neurosci.* **2023**, *17*, doi:10.3389/fncel.2023.1163436.

42. Loufrani, L.; Levy, B.I.; Henrion, D. Defect in Microvascular Adaptation to Chronic Changes in Blood Flow in Mice Lacking the Gene Encoding for Dystrophin. *Circ. Res.* **2002**, *91*, 1183–1189, doi:10.1161/01.res.0000047505.11002.81.

43. Fanin, M.; Nascimbeni, A.C.; Angelini, C. Muscle Atrophy, Ubiquitin-Proteasome, and Autophagic Pathways in Dysferlinopathy. *Muscle Nerve* **2014**, *50*, 340–347, doi:10.1002/mus.24167.

44. Folker, E.; Baylies, M. Nuclear Positioning in Muscle Development and Disease. *Front. Physiol.* **2013**, *4*, doi:10.3389/fphys.2013.00363.

45. Jin, S.; Du, J.; Wang, Z.; Zhang, W.; Lv, H.; Meng, L.; Xiao, J.; Yuan, Y. Heterogeneous Characteristics of MRI Changes of Thigh Muscles in Patients with Dysferlinopathy. *Muscle Nerve* **2016**, *54*, 1072–1079, doi:10.1002/mus.25207.
46. Seror, P.; Krahm, M.; Laforet, P.; Leturcq, F.; Maisonneuve, T. Complete Fatty Degeneration of Lumbar Erector Spinae Muscles Caused by a Primary Dysferlinopathy. *Muscle Nerve* **2008**, *37*, 410–414, doi:10.1002/mus.20910.
47. Yin, H.; Price, F.; Rudnicki, M.A. Satellite Cells and the Muscle Stem Cell Niche. *Physiol. Rev.* **2013**, *93*, 23–67, doi:10.1152/physrev.00043.2011.
48. Schalper, K.A.; Sánchez, H.A.; Lee, S.C.; Altenberg, G.A.; Nathanson, M.H.; Sáez, J.C. Connexin 43 Hemichannels Mediate the Ca²⁺ Influx Induced by Extracellular Alkalization. *Am. J. Physiol.-Cell Physiol.* **2010**, *299*, C1504–C1515, doi:10.1152/ajpcell.00015.2010.
49. Cea, L.A.; Cisterna, B.A.; Puebla, C.; Frank, M.; Figueroa, X.F.; Cardozo, C.; Willecke, K.; Latorre, R.; Sáez, J.C. De Novo Expression of Connexin Hemichannels in Denervated Fast Skeletal Muscles Leads to Atrophy. *Proc. Natl. Acad. Sci.* **2013**, *110*, 16229–16234, doi:10.1073/pnas.1312331110.
50. Samways, D.S.K.; Wolf, K.; Bowles, E.A.; Richards, J.P.; Bruno, J.; Dutertre, S.; DiPaolo, R.J.; Egan, T.M. Quantifying Ca²⁺ Current and Permeability in ATP-Gated P2X7 Receptors. *J. Biol. Chem.* **2015**, *290*, 7930–7942, doi:10.1074/jbc.M114.627810.
51. Kang, J.; Kang, N.; Lovatt, D.; Torres, A.; Zhao, Z.; Lin, J.; Nedergaard, M. Connexin 43 Hemichannels Are Permeable to ATP. *J. Neurosci.* **2008**, *28*, 4702–4711, doi:10.1523/JNEUROSCI.5048-07.2008.
52. Kelley, N.; Jeltema, D.; Duan, Y.; He, Y. The NLRP3 Inflammasome: An Overview of Mechanisms of Activation and Regulation. *Int. J. Mol. Sci.* **2019**, *20*, 3328, doi:10.3390/ijms20133328.
53. Confalonieri, P.; Oliva, L.; Andreetta, F.; Lorenzoni, R.; Dassi, P.; Mariani, E.; Morandi, L.; Mora, M.; Cornelio, F.; Mantegazza, R. Muscle Inflammation and MHC Class I Up-Regulation in Muscular Dystrophy with Lack of Dysferlin: An Immunopathological Study. *J. Neuroimmunol.* **2003**, *142*, 130–136, doi:10.1016/S0165-5728(03)00255-8.
54. Gallardo, E.; Rojas-García, R.; de Luna, N.; Pou, A.; Brown, R.H.; Illa, I. Inflammation in Dysferlin Myopathy: Immunohistochemical Characterization of 13 Patients. *Neurology* **2001**, *57*, 2136–2138, doi:10.1212/wnl.57.11.2136.
55. McNally, E.M.; Ly, C.T.; Rosenmann, H.; Mitrani Rosenbaum, S.; Jiang, W.; Anderson, L.V.B.; Soffer, D.; Argov, Z. Splicing Mutation in Dysferlin Produces Limb-Girdle Muscular Dystrophy with Inflammation. *Am. J. Med. Genet.* **2000**, *91*, 305–312, doi:10.1002/(SICI)1096-8628(20000410)91:4<305::AID-AJMG12>3.0.CO;2-S.
56. Koopman, R.; Schaart, G.; Hesselink, M.K. Optimisation of Oil Red O Staining Permits Combination with Immunofluorescence and Automated Quantification of Lipids. *Histochem. Cell Biol.* **2001**, *116*, 63–68, doi:10.1007/s004180100297.

Disclaimer/Publisher's Note: The statements, opinions and data contained in all publications are solely those of the individual author(s) and contributor(s) and not of MDPI and/or the editor(s). MDPI and/or the editor(s) disclaim responsibility for any injury to people or property resulting from any ideas, methods, instructions or products referred to in the content.